Non-cationic RGD-containing protein carrier for tumor-targeted siRNA delivery

Xiaolin Yu
Augusta University
Lu Xue
the First Hospital of Jilin University
Jingjing Zhao
Second Hospital of Jilin University
Shuhua Zhao
Second Hospital of Jilin University
Daqing Wu
Clark Atlanta University
Hong Yan Liu (hongyl6@uw.edu)
Dotquant LLC, CoMotion Labs at University of Washington

Research Article

Keywords: RGD, siRNA delivery, tumor targeting, tumor neo-vasculature, integrin αvβ3, dsRNA binding domain

Posted Date: June 30th, 2021

DOI: https://doi.org/10.21203/rs.3.rs-643092/v1

Non-cationic RGD-containing protein carrier for tumor-targeted siRNA delivery

Xiaolin Yu[1], Lu Xue[1,3], Jingjing Zhao[2], Shuhua Zhao[2], Daqing Wu[1,4], and Hong Yan Liu[1,5 *]

[1]Georgia Cancer Center, Augusta University, GA 30912 USA. [2]Department of Gynecology and Obstetrics, the Second Hospital of Jilin University, Changchun 130041 China. [3]Department of Pediatrics Hematology, the First Hospital of Jilin University, Changchun 130021 China. [4]Center for Cancer Research and Therapeutic Development, Clark Atlanta University, Atlanta, GA 30314 USA. [5]Dotquant LLC, CoMotion Labs at University of Washington, Seattle, WA 98195 USA

Corresponding author: Dr. Hong Yan Liu. Dotquant LLC, CoMotion Labs at University of Washington, Seattle, WA 98195. Phone: 503-956-5302, email: hongyl6@uw.edu

KEYWORDS: RGD, siRNA delivery, tumor targeting, tumor neo-vasculature, integrin $\alpha_v\beta_3$, dsRNA binding domain

ABSTRACT

Despite the recent successes in siRNA therapeutics, targeted delivery beyond the liver remains the major hurdle for the widespread application of siRNA *in vivo*. Current cationic liposome or polymer-based delivery agents are restricted to the liver and suffer from off-target effect, poor clearance, low serum stability, and high toxicity. In this study, we have genetically engineered a non-cationic tumor-targeted universal siRNA nanocarrier. This protein nanocarrier consists of three function domains: dsRNA binding domain (dsRBD) (from human protein kinase R) for any siRNA binding, 18-histidines for endosome escape, and two RGD peptides at N- and C-termini for targeting tumor and tumor neovasculature. We showed that cloned dual-RGD-dsRBD-18his (dual-RGD) protein protects siRNA against RNases, induces effective siRNA endosomal escape, specific targets on integrin $\alpha_v\beta_3$ expressing cells *in vitro*, and homes siRNA to tumor *in vivo*. The delivered siRNA leads target gene knockdown in the cell lines and tumor xenografts with low toxicity. This multifunctional, biomimetic, charge-

neutral siRNA carrier is biodegradable, low toxic, suitable for mass production by fermentation, and serum stable, holding great potential to provide a widely applicable siRNA carrier for tumor- targeted siRNA delivery.

INTRODUCTION

siRNA has emerged as an invaluable tool for studying gene functions and developing treatment for intractable diseases such as cancer, [1-3] viral infection, [4,5] and genetic disorder.[6,7] Generally, siRNA mediates posttranscriptional gene silencing by targeting and cleaving complementary mRNA. [8-10] The advantage of siRNA over small chemical drugs is that siRNA sequences can be rapidly designed for highly specific inhibition of the target protein expression.[11] siRNA also has advantages over antisense oligonucleotide. In one head-to-head comparison, siRNA knocking down gene expression is about 100-to 1000-fold more efficient than antisense oligonucleotides (ODNs).[12] In 2018, the FDA approved the first siRNA drug (Patisiran), and in 2019, approved the second siRNA drug (Givlaari),[13] suggesting that siRNA drugs are emerging as the third class of medicine after chemical drugs and antibodies for treating diseases by targeting root cause. However, most of siRNA drugs so far have been focused on the liver targeting. Therefore, targeting delivery systems that can deliver siRNA to various target tissues other than liver are needed.

To successfully deliver RNA, vectors should be designed to overcome the barriers such as toxicity, off-target effect, endosomal entrapment, and ease of mass production. However, almost all current siRNA vectors (e.g. lipoplexes,[4] polymers,[14] inorganic nanoparticles,[15] cell penetrating peptide,[16] and micelles [17]) are positively charged, and so are their siRNA complexes. Although cationic carriers facilitate their condensation of negatively charged siRNA, and also enable endosomal escape, cationic carriers can interact with negative charged serum components, form unstable complexes in the circulation system, and cause off-target effect.[18,19] Additionally, inorganic nanoparticles and polymers have serious safety concerns due to non-degradable and poor clearance. Therefore, current vectors are unsuitable for systemic delivery of siRNA. In our previous studies, we have developed an innovative technology for aptamer-siRNA delivery by engineering a non-cationic protein-based

carrier (dsRBD-18 His).[20] Our small protein carrier was developed by adding 18 Histidine (His) peptide on a dsRNA binding domain (dsRBD) protein from human protein kinase R (PKR). DsRBD protein enables binding to dsRNA via specific 3-D conformation but not via charge-charge interaction. [21,22] His molecules have pKa value about 6, at neutral pH, they are uncharged, and charged in acidic condition such as endosome. We have proved that 18His are capable of providing sufficient buffering capacity to drive cargo endosomal escape.[20] Other studies also showed that addition of 2 His into protein has enhanced endosomal escape,[23] and two His mutations increase the engineered Her2 targeted antibody drug lysosomal delivery.[3] Notably, siRNA/dsRBD complexes are able to protect siRNA from degradation by ribonucleases.[24] Our developed dsRBD-18 His protein can binding siRNA and enables siRNA endosomal escape.

However, all current siRNA vectors including dsRBD-18His do not have cell-type specificity, and targeting molecules such as aptamer, antibody or ligand must be added onto siRNAs. That conjugation process is time-consuming and restricts siRNA application *in vivo.*

In this study, we have developed a universal tumor-targeted siRNA vector by fusing RGD (Arginine-Glycine-Aspartic Acid) peptide into dsRBD-18His protein. RGD has high affinity and specificity on integrin $\alpha_v\beta_3$, which is highly expressed on tumor neovasculature endothelial cells and many tumor cells, but not presents in resting endothelial cells and normal organ systems. RGD peptide is a well validated tumor targeting molecule and has been used for guiding imaging agents[25-27] and drugs[28-30] for tumor diagnosis and therapy in clinical setting. Our cloned RGD and 18His- containing protein vector with load-to-go capability will simplify siRNA delivery *in vivo* and enables delivering a wide range of siRNAs to many tumors and tumor microenvironment. To increasing binding efficacy, we have cloned two RGD domains flanking on dsRBD-18His protein both sides.

RESULTS

Construction and expression of dual RGD-dsRBD-18His (dual-RGD) recombinant protein. In our previous studies, we have cloned a dsRBD-18 His protein which contains a double stranded RNA binding domain and 18His.[20] In this study, we have genetically engineered two RGD peptides into N- and C- termini of dsRBD-18His protein, respectively. N-terminal of dsRBD-18His was appended a cyclic RGD peptide (CDCRGDCFC (RGD-4C)). RGD-4C has been cloned with TNFα and tumor necrosis factor-related apoptosis-inducing ligand (TRAIL). RGD-4C-containing TNFα and TRAIL have shown strong tumor selectivity and binding affinity, and also keep natural activities of TNF [31] or TRAIL [28]. Meanwhile, C-terminal of dsRBD-18His was added a G**RGD**S (Gly-Arg- Gly-Asp-Ser) peptide since G**RGD**S is relative conserved in natural RGD-containing proteins such as fibronectin and α-lytic protease.[32,33] The gene structure of dual-RGD was illustrated in **Figure 1A**. Briefly, dsRBD-18His gene in PET28a plasmid[20] was selected as cloning PCR template. RGD genes and BamH1/Xhol1 restriction enzyme recognition sites were introduced at the 5'-and 3'- end of primers, respectively. The recombinant protein was expressed in *E.coli* BL21(DE3) induced by 1mM of IPTG. Expressed protein was purified by Ni-NTA affinity column. The purified protein was analyzed on SDS-PAGE with Coomassie blue staining. As shown in **Figure 1B**, there are two high density bands in the non-reducing condition (Lane 2). After adding β-mercaptoethanol (β-ME) and experiencing heating, the larger size protein disappeared, and small size protein remains (Lane 3), that indicates dual-RGD protein can form homodimer under nonreducing condition. SDS-PAGE with molecular weight (MW) marker shows the expected molecular weight of ~ 26kDa

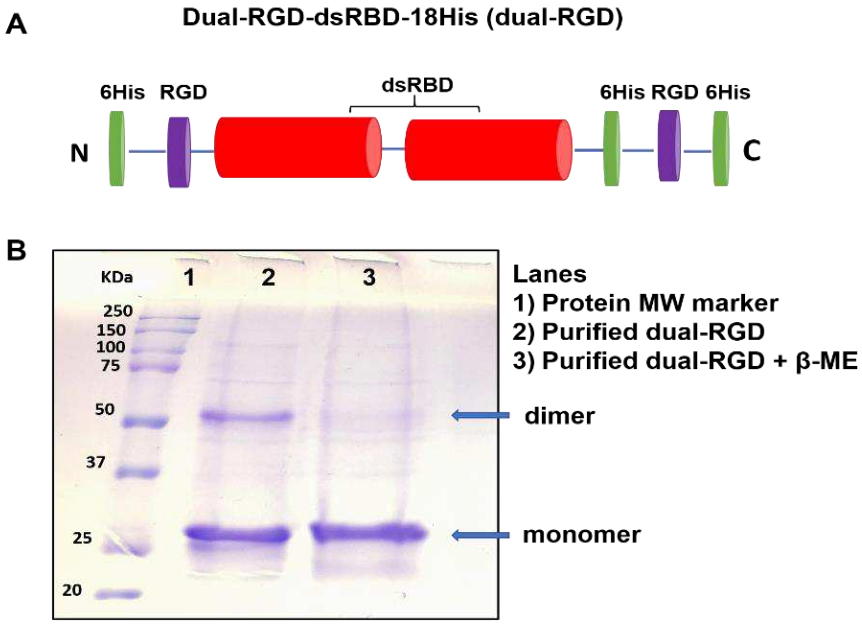

Figure 1. Cloning and production of dual-RGD-dsRBD-18H (dual-RGD) protein. (A) Schematic illustration of dual-RGD protein structure. (B) SDS-PAGE analysis of dual-RGD protein. Dual-RGD protein is shown as monomer (26KDa) and dimer (52KDa) on nonreducing condition (lane 2) and a single monomer under reducing condition (lane3). The full- length gel is presented in Figure S2.

(monomer) and ~ 52kDa (dimer). Based on above protein conformation, in the following protein purification, we have added β-ME to keep dual-RGD protein as a monomer for function characterization.

siRNA binding capability. Next, we have evaluated the functionalities of three domains in dual-RGD protein including dsRBD, 18His, and RGD. First, we have detected dsRBD domain for siRNA binding. Selected as a siRNA model, EGFR siRNA was labeled with FAM fluorophore at 5'-end of sense strand. FAM-labeled EGFR siRNA was incubated with dual-RGD at different protein/siRNA molar ratios (1:1, 2:1, 4:1) for 30 min at room temperature. Bound and unbound siRNA was quantified on 1% agarose gel electrophoresis. As shown in **Figure 2A left**, under UV transilluminator, the mobility of complex of siRNA & dual-RGD was much slower than control of siRNA only. At 1:1molar ratio, all of siRNA has bound to dual-RGD and no free siRNA is detectable. To further detect if slowly moving siRNA has indeed bound to dual-RGD protein during the migration, the same gel was stained with Coomassie blue to identify the location of dual-RGD protein. As shown in **Figure 2A right**, the bright field image shows the protein location (Coomassie blue) is colocalized with siRNA location (UV revealed). The result clearly indicates that dsRBD domain in dual-RGD maintains siRNA binding capability. In the previous studies,[34] with cognate HIV TAR RNA (59NT) that contains bulges and internal loop, using isothermal titration calorimetry, the interaction of TAR RNA with dsRBD was fit a model for two binding sites in TAR. One is a single high affinity

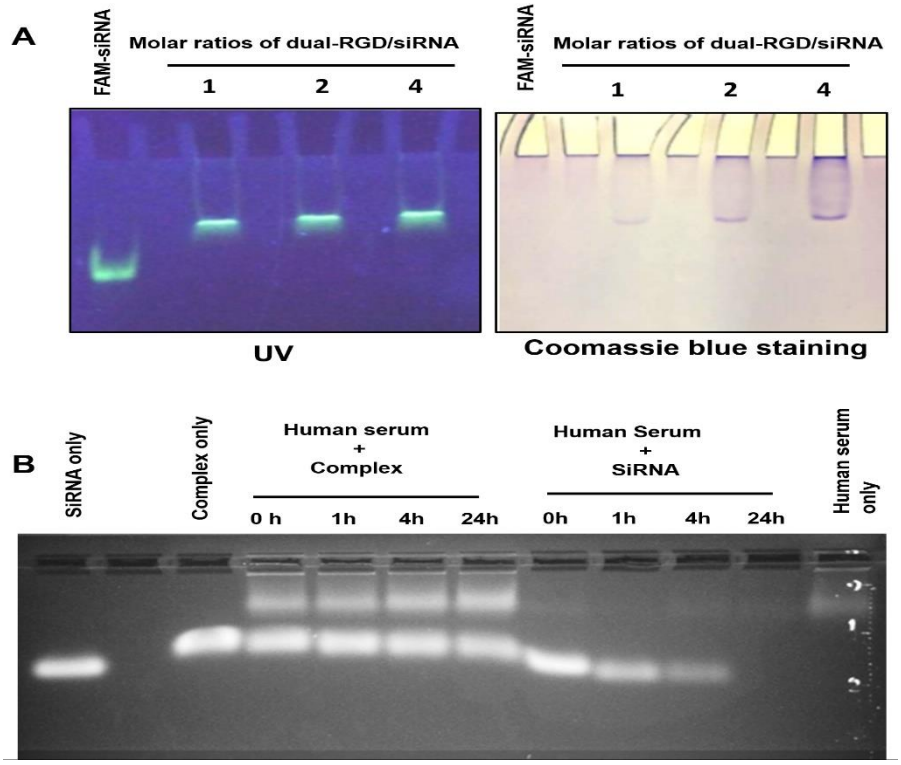

Figure 2. Characterization of dual-RGD on binding and protection of siRNA. (A) Gel retardation to assess dual-RGD/siRNA binding. FAM-labeled siRNA was incubated with different molar ratios of dual-RGD protein. The complexes were detected by 1% agarose electrophoresis. SiRNA migration location was imaged under UV transilluminator. To localize dual-RGD protein position, the same gels were stained with Coomassie blue. Two images show that dual-RGD and siRNA are at the same location that indicates dual-RGD binding to siRNA. The full- length gel is presented in Figure S3. (B) Protection of siRNA against nucleases. Naked siRNA or siRNA/dual-RGD complexes were incubated with 50% (v/v) human serum for the different time periods at 37° C. The siRNA degradation was probed with agarose gel electrophoresis. The full-length gel is presented in Figure S4.

site and the second is a low affinity site. At 1:1 molar ratio of dsRNA to dsRBD. a type 1 complex with a fast gel mobility will be formed. At higher ratios 1:2, a type 2 complex will be formed with slow gel mobility. The dissociation constant for the type 1 complex is 70nM with a 1:1 stoichiometry. In the contrast, the dissociation constant for the type 2 complex is 23μM with 1:2 stoichiometry which is 300-fold higher than type 1 complex. Importantly, the previous studies,[22] also demonstrated: 16-20 bp dsRNA binding to dsRBD resulted in formation only complex 1 at 1:1 molar ratio; while 22-24 bp dsRNA binding to dsRBD can form complex 2 at molar ratio 1:2 of dsRNA to dsRBD . In our report, we only observe complex 1 (1:1 molar ratio) (Figure 2A) because our siRNAs are 19bp.[35] Our results are in agreement with previous studies. Meanwhile, Complex 1 will have smaller size than complex 2 that will be suitable for tissue penetration in vivo.

Protection of siRNA against nucleolytic degradation. Following confirmation of dual-RGD/ siRNA binding, we evaluated if the formation of complexes could protect siRNAs from RNase attack**.** Dual-RGD /siRNA complex or siRNA only was spiked with 50% fresh pooled human serum at the different time. As shown in **Figure 2B**, siRNA in complexed with dual-RGD did not show degradation for 24-h test period, while siRNA alone in 50% human serum has shown degradation in the start 1h. Therefore, dual-RGD carrier could protect siRNA against nuclease digestion. Notably, we did not do chemical modification for the test EGFR siRNA. The serum volume always accounts for 50% (v/v) in all test groups. Thus, it is not surprising that serum volume in siRNA alone groups is lower than that in siRNA/dual-RGD complex groups since siRNA alone has lower volume than siRNA/dual-RGD complex (**Figure 2B**).

RGD binding specificity. Binding specificity of dual-RGD protein was assessed in a series of cell lines with different levels of integrin $\alpha_v\beta_3$. To verify the expression levels of integrin $\alpha_v\beta_3$, different cell lines were probed for integrin β_3 expression with Western blot. As shown in **Figure 3A**, cell lines of MDA-MB-231, Hs587T and BT20 express high level of integrin β_3, while cell lines of C4-2, BXPC3 and HEK293T show very low expression level of integrin β_3. Next, FAM-EGFR siRNA was loaded into dual-RGD at molar ratio 1:1. Complex of dual-RGD/siRNA was incubated with formalin fixed cell lines at 37 ºC for 1h, and the binding specificity of dual-

RGD was detected by flow cytometry. Notably, fixed cells will allow RGD binding to target cells but not inducing endocytosis, thus will provide precise assessment of cell surface integrin receptor-RGD binding. As shown in **Figure 3B**, dual-RGD has low or none binding to C4-2 and HEK-293T cells, while has high binding intensity for MDA-MD-231, Hs578T and BT-20. The correlation of single-cell fluorescence intensity and integrin β_3 protein levels demonstrated the binding specificity of RGD domain in dual-RGD protein. Furthermore, in another independent experiment, competitive binding assay was performed to evaluate RGD-receptor specific binding. MDA-MB-231 cells were incubated with dual-RGD/siRNA in the present of free RGD peptide. As shown in **Figure 3C**, after blocking with RGD peptide, the binding intensity of dual-RGD/siRNA to MDA-MB-231 cells was significantly reduced which is displayed by the fluorescence peak significant shifting to the left. Above experiments suggest that the binding of dual-RGD/siRNA complex to the cells is indeed through fused RGD domain in dual-RGD carrier.

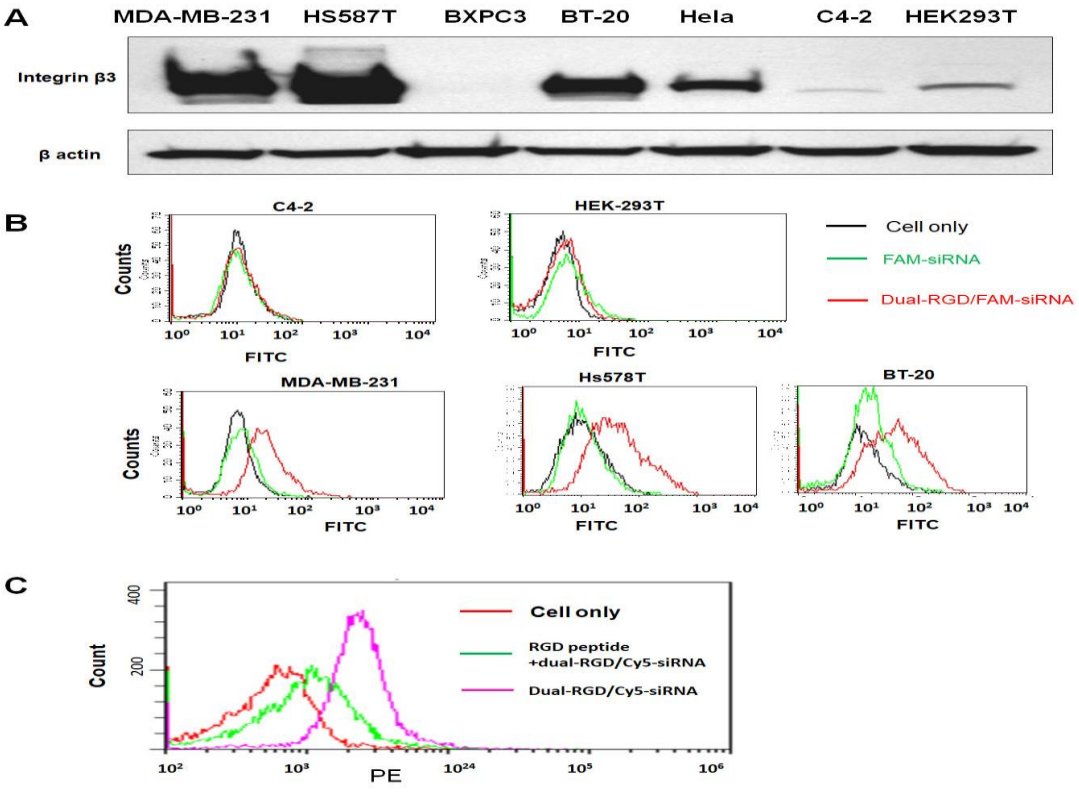

Figure 3. Integrin $\alpha_v\beta_3$ binding specificity. (A) Detection of integrin β_3 expression levels in cell lines by Western blot. The full blot is presented in Figure S5. (B) Evaluation of dual-RGD cell-type-specific binding by flow cytometry. FAM-siRNA/dual-RGD or FAM-siRNA only was incubated with formalin -fixed cell lines at 37 ℃ for 1h, and the binding specificity of dual-RGD was detected by flow cytometry. (C) Competitive assay. Fixed cell lines were first treated with free RGD peptide, and then Cy5-siRNA/dual-RGD complexes were added to the cells. The binding intensity was detected

Cellular uptake and subcellular distribution of dual-RGD carrier. Furthermore, we assessed if RGD-integrin binding has induced cell-type specific internalization and endosomal escape which is the prerequisite of siRNA triggering gene silencing. In this recombinant protein, dual-RGD was incorporated with 18His which is expected to provide endosomal rupture through proton sponge effect. To prove 18His endosomolytic activity, confocal microscopy was performed to visualize the subcellular location of siRNA. First, Cy5 (red) fluorophore labeled siRNA was complexed with dual-RGD or dsRBD-18His (without RGD targeting moiety as control) at molar ratio of 1:1. Then integrin $\alpha_v\beta_3$ positive MDA-MB-231 live cells were treated with siRNA/dual-RGD or siRNA/dsRBD-18His for 6 h in 37 ℃ at CO2 incubator followed by DPBS wash. In the meantime, nuclei were labeled with DAPI (blue), and endosome/lysosomes were stained with Lysotracker (green). As shown in **Figure 4 (the top and middle layers**), siRNA/dual-RGD treated MDA-MB-231 cells showed the much higher density of red fluorescence signal in cytoplasm compared with siRNA/dsRBD-18His treated control. It is worth mentioning, the yellow fluorescence signal is derived from the colocalization of Cy5-siRNA (red) with Lysotracker (green) and indicates siRNA endosomal entrapment. In siRNA/dual-RGD-treated MDA-MB-231 cells, low amount yellow fluorescence signal indicates less Cy5-siRNA was entrapped in endosomes, and high amount red signal in cytoplasm around nuclei indicates most siRNA has escaped from endosomes. Above results suggested that cloned RGD peptide can led receptor-mediated endocytosis, and internalized siRNA can escape from endosome and diffuse to cytoplasm. Furthermore, as cell type control, integrin $\alpha_v\beta_3$ negative C4-2 cells were treated with Cy5-siRNA/dual-RGD for 6 h and washed with DPBS. The confocal image (**Figure 4 bottom layer**) showed that there is no detectable Cy5-siRNA signal in C4-2 cells, that is consistent with binding specificity assay shown in **Figure 3**. These results strongly implied that dual-RGD directed siRNA endocytosis is cell-type specific that may avoid off-target effect during *in vivo* circulation.

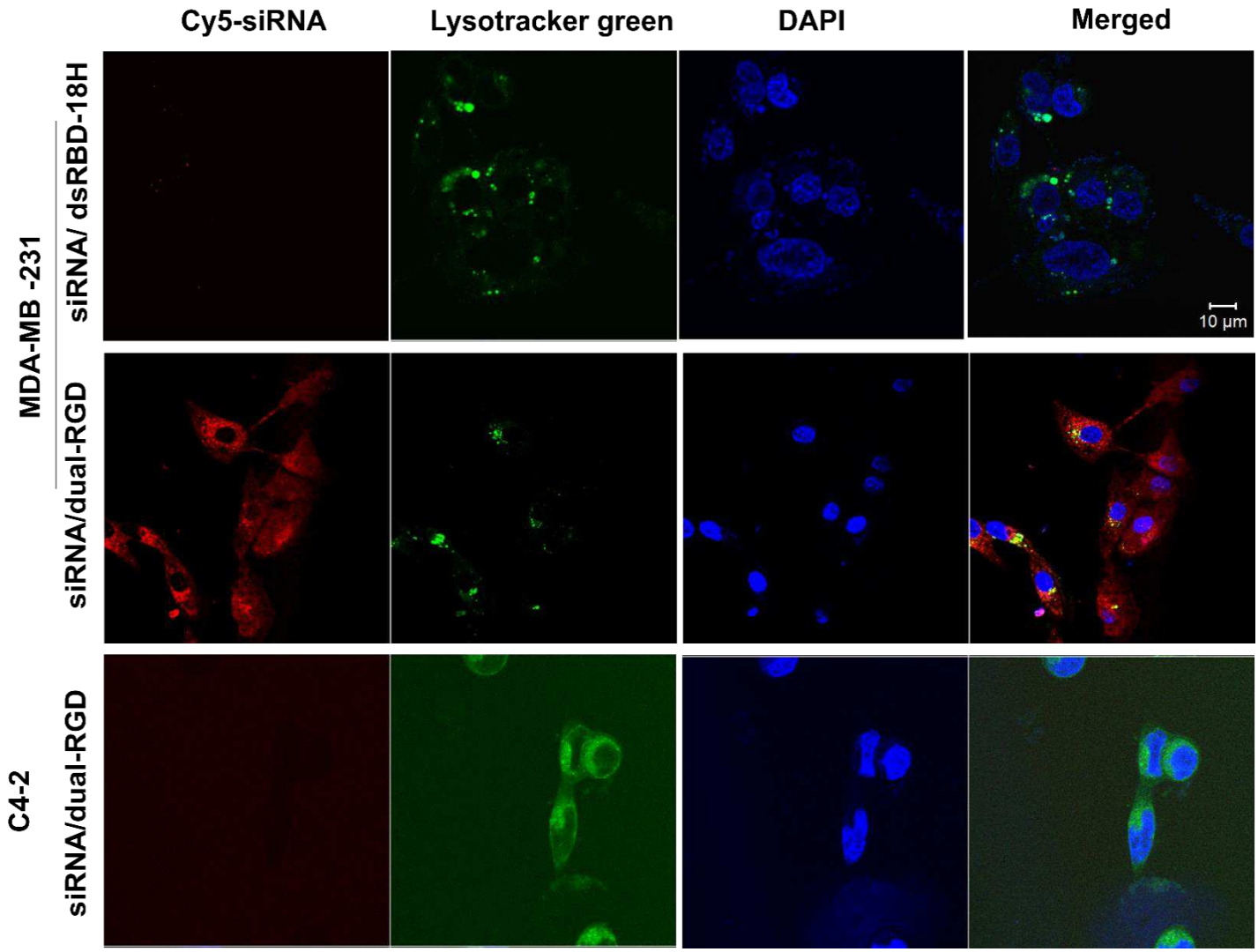

Figure 4. Detection of dual-RGD/ Cy5-siRNA internalization by confocal microscopy. The complexes of Cy5-siRNA /dual-RGD were incubated with MDA-MB-231 (integrin $\alpha_v\beta_3$ positive) and C4-2 cells (integrin $\alpha_v\beta_3$ negative), and Cy5-siRNA complexed with dsRBD-18H without RGD as protein control were incubated with MDA-MB-231 cells. Lysotracker Green (green) was used to show endosomes and lysosomes, and DAPI (blue) was used to display nucleus. Confocal laser scanning microscopy images were acquired after treatment. Scale bar, 10µm.

Target gene knockdown *in vitro*. After confirmation of dual-RGD led siRNA endocytosis and endosomal escape, we evaluated if siRNA has triggered target gene knockdown. As a model, EGFR siRNA was selected and formed complexes with dual-RGD at molar ratio of 1:1. EGFR siRNA/ dual-RGD complexed were incubated with MDA-MB-231 cells or Hs587 T cells for 72 h. It is worth mentioning, both MDA-MB-231 and Hs587T cells have high EGFR expression reported in our previous studies. [36] Cationic lipofectamine RNAi MAX was used as a control to verify siRNA functionality. The gene knockdown were probed in cell lysates with Western

blot. As shown in **Figure 5**, dual-RGD/siRNA complex displyed a dose-dependent gene knockdown in both cell lines. At 200nM, siRNA/dual-RGD can silence 85% EGFR in MDA-MB-231 cells and 75% of EGFR in Hs578T cells. It is not surprising that lipofectamine RNAi MAX show better peformance. However, siRNA uptake by cationic lipofectamine is via charge-charge interaction between lipofectamine (cationic) and charged cell membrane (anionic). Since cellular uptake through charge-charge interaction has no cell type specificity, lipofecatime is incapable for *in vivo* siRNA taregting delivery.

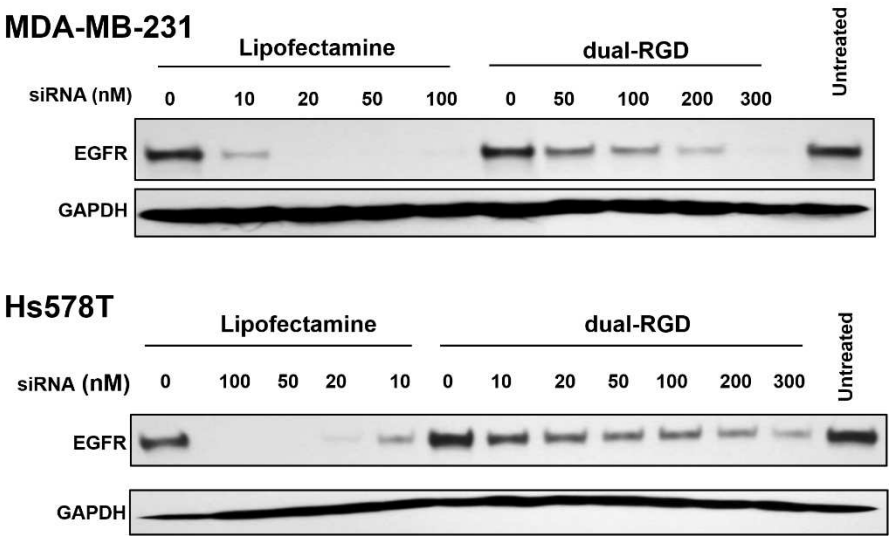

Figure 5. Detection of in vitro target gene knockdown. Integrin $\alpha_v\beta_3$ expressing MDA-MB-231 and Hs578 T cell lines were treated with EGFR siRNA/dual-RGD at varying concentrations for 72 h. Lipofectamine was selected as a control. After treatment, the cell lysates were probed by Western blot. The full blots are presented in Figure S6.

Tumor-targeting capability *in vivo*. After confirming the functionalities of three domains of dual-RGD protein *in vitro*, we further evaluated it *in vivo*. MDA-MB-231 tumor-bearing mice were intravenously (iv) injected with 100µl of Cy5-EGFR siRNA/dual-RGD complex (5 nmoles) or equal moles of Cy5-siRNA/dsRBD-18His complex control. At time points of 3h, 6h, 12h and 24h, Cy5 fluorecence signal in mice were detected with Xenogen IVIS100 imaging system to monitor siRNA distribution in whole body (**Figure 6**). After 3h-injection, Cy5 siRNA signal can be detected in the tumors of dual-RGD treated mice but not in the tumors of dsRBD-18His treated mice. At 6-h time point, Cy5-siRNA in dual-RGD treated mice can be clearly visualized in tumors but with the reduced signal around other organs, whereas Cy5-siRNA in dsRBD-18His treated mice keeps undetectable in tumors. Cy5-siRNA signal in tumors can last to 12 h in dual-RGD treated mice. After 24 h, both dual-RGD and dsRBD-18his delivered Cy5-siRNA have been removed from mice. This results indicate dual-RGD enables delivering siRNA to tumor sites where siRNA can stay for 12 h. Since we have labeled siRNA sense strand with Cy5, it is possible the sense strand (passenger strand) of siRNA was degraded after loading

into RISC (the RNA-Induced Silencing Complex) followed by gene silencing that is a natural process for RNA interference but not serum nuclease-induced degradation. The time-course imaging demonstrated that dual-RGD can guide siRNA targeting tumors *in vivo*. After 24 h, we removed the major organs in dual RGD treated mice, as shown in Supplement Figure S1, there are olny weak fluorence signals in the sites of intestine/stomach and the brain (around eyes), most organs including heart, lung, kidney, spleen and liver are free of Cy5 signals. We reason that capillary blood vessels around eyes have slow metabolic rate than other organs and intestine/stomach may experience the process of removing all metablites, thus some signals were detected in these organs.

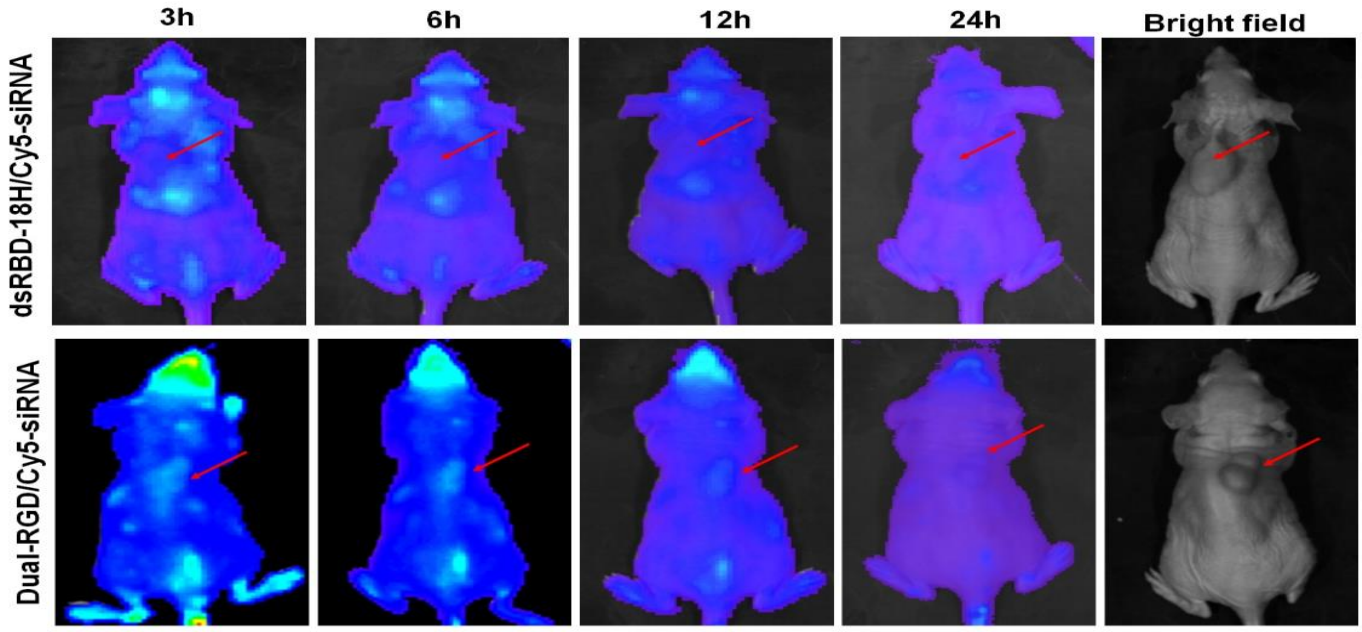

Figure 6. Time-course imaging of Cy5-siRNA/dual-RGD in vivo biodistribution. MDA-MB-231 tumor bearing mice were iv treated complexes of Cy5-siRNA/ dual-RGD or Cy5-siRNA/dsRBD-18His. Biodistribution was captured with Xenogen IVIS 100 system. Red arrows indicate tumor sites.

Target gene knockdown *in vivo*. Furthermore, target gene knockdown was assessed in MDA-MB-231 xenografts. When tumors reach 100mm^3, mice were *iv* treated with EGFR siRNA/dual-RGD (5nmoles) or controls of saline, EGFR siRNA, EGFRsiRNA/dsRBD twice a week for 4 weeks. At the endpoint, tumors and major organs were removed. Tumors were analysed by IHC and Western blot. As shown in **Figure 7**. IHC has demonstrated the signficacnt reduced expression in siRNA/dual-RGD group, but not in control groups of saline, siRNA only, and siRNA/dsRGD-18His. Western blot assay with tumor cell lysate proved the down regulation of

EGFR protein. ImageJ quantitation indicates that after 4-week treatment, only 30% of EGFR protein remained. These results indicate that taregt gene has been signficantly knocked down *in vivo.*

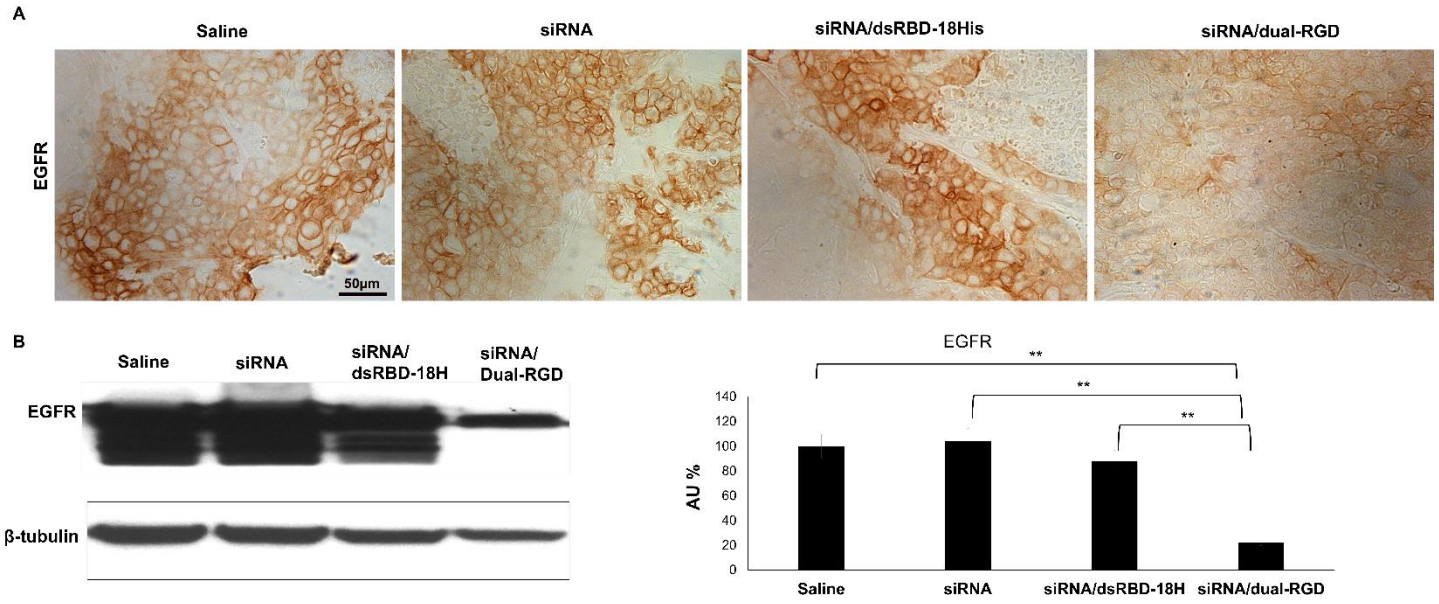

Figure 7. Evaluation of target gene knockdown in vivo. MDA-MB-231 cell xenografts were treated with EGFR siRNA/dual-RGD or controls twice a week for four weeks. (A) EGFR expression was detected by IHC. Formalin-fixed paraffin-embedded sections of xenograft tumors were stained with anti-EGFR antibodies compared with controls of saline, siRNA, siRNA/dsRBD-18His. Scale bar, 50μm. (B) Tumor EGFR protein expression was measured by Western blot. Quantification of protein levels normalized by GAPDH using imaging J. The results are the pool of three mice per group. P^{**} <0.01. The full blot is presented in Figure S7.

Toxicity assessment. Next, we evaluated the possible cytotoxicity of dual-RGD to intergin $\alpha_v\beta_3$-negative cells. Since RGD as a drug has shown cytotoxicity for intergrin $\alpha_v\beta_3$ expressing tumor cells, [37,38] we would like to find if dual-RGD protein will have cytotoxicity to intergin $\alpha_v\beta_3$-negative cells. Intergin $\alpha_v\beta_3$-negative C4-2 and HEK293T cells were selected and treated with the varying concentrations of dual-RGD carrier for 72h, then CCK-8 reagent were added to detect cell viability. As shown in **Figure 8**, both C4-2 and HEK293T cells have kept over 92% cell viability after treated with 0.2-1.0 μM of dual-RGD carrier protein. The results showed that there are no significant toxicity in the detection range up to 1.0μM that is three times as high as the one used in the delivery work.

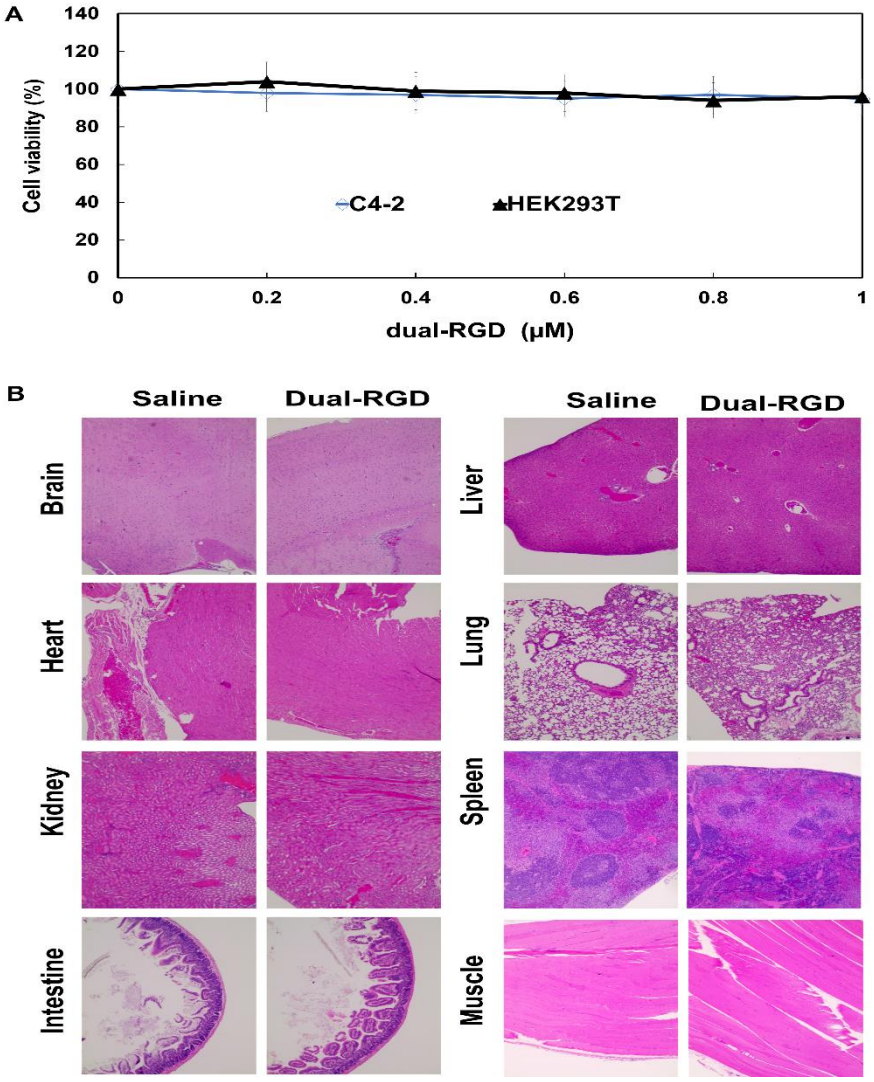

Figure 8. Assessment of toxicity. (A) Cell viability assay. Integrin $\alpha_v\beta_3$ negative C4-2 and HEK293 cells were treated with the varying concentrations of dual-RGD for 72h. CCK-8 reagent was added into each well for 4 hours. Absorbance was measured at 450nm. (B)Histology examination of dual-RGD on major normal organs. Athymic mice were treated with dual-RGD or saline for four weeks. After treatment, the major organs were fixed and stained with H&E. Images were captured under 20x magnification microscopy.

Furthermore, we evaluated the possible toxicity *in vivo*. After mice were *iv* treated with dual-RGD protein or saline twice a week for 4 weeks, majors organs including brain, heart, kidney, liver, lung, intestine, muscle and spleen were collected and examined the histopathology changes. As shown in Figure 8A, H&E staining revealed that there is no discernible abnormality observed in dual-RGD protein treated groups compared with saline-treated control. These results suggest that human origin dual-RGD protein carrier is biocompatible and show none to low systemic toxicity *in vivo.*

DISCUSSION

Tumor-targeted siRNA delivery is of great interest in medicinal research. It is highly desirable but technically challenging to engineer efficient vectors featured with non-cationic, non-toxic, endosomal escapable, cell-type specific, and ease of mass production. To find a carrier for *in vivo* systemic siRNA delivery, natural human

proteins are attractive because they are biocompatible, biodegradable, and easy clearance from body, and ease of mass production by fermentation.

Human PKR has been extensively studied[24,39] as a natural carrier for *in vivo* siRNA delivery. Natural PKR in body is activated by dsRNA and plays a major role in the cellular antiviral response through inhibition of eukaryotic initiation factor 2 (eIF-2). [40 41] PKR consists of an N-terminal dsRBD including a pair of double-stranded RNA binding motifs (dsRBM1, and dsRBM2)[42,43] and a C-terminal kinase domain[44]. dsRBM1 has a dominant role in molecular recognition of short dsRNA sequences (15-30 bp), whereas both motifs contribute to binding longer dsRNA sequences (>40bp). dsRBD binds RNA though protein 3-D conformation but not through charge-charge interaction.[21] In addition to its ability to sense dsRNA, primarily of viral origin, PKR is also activated in response to endogenous RNA such as microRNAs . [45,46] DsRBD from PKR can bind to a broad range of dsRNA in a sequence-independent manner [47] which is unique among known RNP (ribonucleoprotein) complexes. It also has been proved that dsRBD only binds to dsRNA but not RNA-DNA hybrids or dsDNA, [22] that provides the basis to generate dsRBD as siRNA carrier. However, dsRBD lacks endosomal escape capability. To address this problem, we have used polyhistidine as an endosomal escape moiety instead of peptide transduction domains (PTD) because PTD also is an arginine- and lysine-rich positive-charged peptide. Histidine has pKa value about 6.0, at neutral or tumor environment (pH6.5-6.9) condition, [48] they are mainly deprotonated (uncharged), while in acidic condition such as late endosome (pH 4.5-5.5),[49] histidine becomes protonated (charged) and facilitates osmotic swelling leading to cargo release, a mechanism proposed as the proton sponge effect.[50] However, it is well known that 6xHis tag used for protein purification has not demonstrated the capability of endosome escape. We reason that 6xHis is too short to offer enough buffering effect, and certain elongated His tag should confer cargo endosomal escape. We have inserted 18 His peptide into dsRBD protein.[20] We have compared endosomal escape capability of dsRBD-18His and dsRBD-6His. Our results demonstrated that adding 12 more His can significantly improve endosomal escape capability. 18His can confer adequate buffering capacity to drive cargo endosomal escape. In contrast to cationic carriers, dsRBD-18His is uncharged at the physiological

condition, low toxic, and biodegradable. Based on dsRBD-18His vector, we have further equipped it with two RGD peptides for tumor targeting.

The mechanism of siRNA released from dsRBD is believed via displacement by the highly abundant longer RNA molecules in cytosol.[51] Since dsRBD recognizes RNA in a sequence-independent fashion, in the referred studies, with total RNA isolated from cells, dsRBD-siRNA complex was incubated with 80ng/μl cellular RNAs (which is still much lower than the cytosolic RNA concentration), the siRNA-dsRBD complex is totally disrupted. Their studies support that the competitive binding and exchange of cellular RNAs to dsRBD can trigger siRNA release from dsRBD inside of cells.

In this study, we aim at establishing a general tumor-targeted siRNA delivery platform. We have focused on characterization of dual-RGD performance *in vivo* and *in vitro*, and we will evaluate tumor treatment efficacy in the next study. RGD peptides have been widely used in the drug delivery and imaging and has defined minimized safety concerns.[26,52] RGD has high affinity and specificity on integrin $\alpha_v\beta_3$, which is highly expressed on tumor new blood vessels and many tumor cells, but not present in resting endothelial cells and normal organ systems. New RGD carrier will simplify the process of siRNA delivery and enable targeting delivery of siRNAs to tumor blood vessels and many tumors such as glioblastomas, melanomas, pancreatic, ovarian, breast and prostate cancers. [53-55] RGD-based materials have undergone rapid development for sensitive tumor detection and tumor targeted drug delivery *in vivo*.[23,56,57] RGD-PET (positron emission tomography) has been used in the clinic for tumor diagnosis[58,59] . RGD also has been widely used in developing anti-angiogenesis therapeutics, [60,61] and conjugating with radionuclides [62,63] or chemotherapeutic drugs [64,65] for tumor treatment. TNFα has been fused with RGD by recombinant DNA technology and achieved targeting tumor and reducing system damage. [66,67] Cyclic RGD peptide has shown better targeting capability *in vivo*. In this study, to avoid unwanted internal disulfide bonds between N- terminal and C- terminal, we have cloned one end (N-) with cyclic RGD and another end (C-) with linear GRGDS peptide. The results proved that the cloned protein possesses ideal functionality.

In terms of delivery efficacy, lipofectamine outperforms dual-RGD carrier. This is expected since cationic charge-charge interaction between lipofectamine and cell membrane is much effective in gene transfection than ligand-receptor mediated endocytosis which is the way of dual-RGD carrier assumed. However, cationic lipofectamine cannot be used *in vivo* due to nonspecific binding and cytotoxicity.

Cyclic peptide c(-RGDfV-), as a drug Cilengitide, has shown the inhibition of tumor growth and angiogenesis.[37,38] We envision fusion protein dual-RGD carrier complexed with siRNA will have increased anti-tumor efficacy in addition of siRNA induced gene silencing.

CONCLUSION

Our developed protein-based dual-RGD vector has three functions: dsRBD domain for siRNA docking, 18 His for endosomal escape, and RGD for tumor targeting. This three-in-one multidomain vector will address the problems of current siRNA carriers in positive charge, low serum stability, poor clearance, cytotoxicity, and lack of cell type specificity. Our cloned dual-RGD protein carrier with load-to-go capability will expedite siRNA translation to *in vivo* tumor therapy.

MATERILAS AND METHODS

Materials. Cell culture products were purchase from Gibco through Thermo Fisher Scientific (Waltham, MA). Cell lines were purchased from the Americn Type Culture Collection (ATCC, Manassas, VA). PET28a plasmid, Bug-Buster mix, Ni-charged His Bind resin and *E.coli* BL21 (DE3) competent cells were ordered from Novagen/ MilliporeSigma. Restriction enzymes and Taq polymerases were obtined from New England Biolabs. Antibodies were ordered from Cell Signalining Technology (Danvers, MA). siRNAs and fluorophore-labeled siRNAs were ordered from Dharmacon/Horizon Disocvery (Lafayette, CO). LysoTraker Green DND-26 were from invitrogen (Carlsbad,CA). Cell Counting Kit-8 reagent was ordered form Dojindo Molecular Technologies (Rockville,MD).

Mouse. All animal studies were approved by the Institutional Animal Care and Use Committee at Augusta University. Athymic nu/nu mice were purchased from Harlan Laboratories, Inc. The methods were carried out in accordance with the approved guidelines. The studies were carried out in compliance with the ARRIVE guidelines.

Construction of fusion protein dual-RGD (dual-RGD-dsRBD-18His) expression plasmid. The dsRBD-18His-containing plasmid was used as PCR template. For amplification by PCR, the primes were used: Forward 5'- AAA**GGATCC** ATG TGT GAT TGT CGT GGA GAT TGT TTC TGT GGTAGT GCTGGTGAT CTTTCAGCAG-3', Reverse 5'-TT**CTCGAG**GCTGTCTCCACGGCCGTGGTGGTGGTGGTGGTGCACTG AG GTTTCTTCT-3'. BamH1 and Xho1 recognition sites were introduced in the primers and bolded. PCR product and PET28a plasmid were digested with BamH1 and Xho1. After digestion, PCR fragment was inserted into PET28a by T4 DNA ligase. Ligates were transformed into *E.coli* BL21 (DE3) competent cells. The positive clones were confirmed by gene sequencing.

Expression and purification of dual-RGD recombinant protein. Positive colonies were selected and grown at 37ºC in LB medium containing kanamycin (30 µg/ml). When the OD_{600} reaches 0.4-0.6, protein expression was induced by isopropyl-β-D-thiogalactopyranoside (IPTG,1 mM) for 4 h at room temperature. Cells were harvested by centrifugation at 10,000 g for 10 min and the pellet was stored at -20 ºC. To isolate the soluble proteins, the cell pellet was lysed by the Bug-Buster Mix in the presence of a protease inhibitor EDTA-free cocktail. The cell lysate was centrifuged at 20,000g for 20 min at 4ºC to remove insoluble cell debris. The soluble extracts were loaded onto a Nickle Resin column and eluted with the His•Bind® Buffer. The eluted protein was dialyzed against PBS containing 10% glycerol and 0.1% (v/v) β-ME for 24 h. Protein concentrations was determined with the Bio-Rad Protein Assay using BSA as the standard. Purified protein was probed using SDS-PAGE.

SiRNA binding assay. To assess siRNA binding capability of dual-RGD carrier, a gel retardation assay was performed. EGFR siRNA was labeled with FAM fluorophore at the sense strand 5' end. FAM-siRNA was incubated with dual-RGD at different protein/siRNA molar ratios (1:1, 2:1, 4:1) for 30 min at room temperature. Bound and unbound siRNA was quantified on 1% agarose gel electrophoresis. Images first were captured under UV transilluminator. Then the same gel was stained with Coomassie blue to reveal protein location and stained gel was imaged again under bright light.

RNase resistance and serum stability. siRNA was labeled with FAM at the sense stand 5' terminus. dual-RGD /siRNA complex or siRNA only was spiked with 50% (v/v) fresh pooled human serum at the different time (1h, 4h, 24h). 1% Agarose gel electrophoresis was performed to monitor the dissociation.

Western blot. Cell lysates or tumor tissues were lysed in lysis buffer (M-PER Mammalian Protein Extraction Reagent, Thermo Fisher Scientific) containing 1x Halt Protease Inhibitor Cocktails. The cell lysates were kept on ice for 40 min and vortexed for 3 times and centrifuged at 12,000 × g for 10 min at 4 °C. The concentration of supernatant protein was determined with Bio-Rad Protein Assay. Samples were separated on 8 % SDS-PAGE and transferred to PVDF membrane. The membranes were blocked with 5% non-fat milk, and then incubated with primary antibodies for 2 h at room temperature followed by incubation with HRP-conjugated secondary antibodies for 2 h at room temperature. After ECL Western Blotting Substrate (Pierce) was added onto membrane, the signals were captured by the exposure to X-ray film. Western blot was quantified using ImageJ (NIH).

Cell-type specific binding assay. Cell lines with different integrin $\alpha_v\beta_3$ expression levels were grown to 80% confluence and trypsinized from dishes. Collected cells were fixed in 10% buffered formalin for 30min. siRNA sense strand was labeled with fluorophore FAM or Cy5 at the 5'end. FAM-siRNA (5nmoles of siRNA) was loaded into dual-RGD at molar ratio 1:1. Complex of dual-RGD /FAM-siRNA was incubated with fixed cell lines at 37 ºC for 1h, and the binding specificity of dual-RGD was detected by flow cytometry (BD FACSCalibur Cell

Analyzer). In the competitive assay, RGD peptide (10 nmoles) was treated cells for 1h before adding complex of dual-RGD/Cy5-siRNA.

Cellular uptake and endosomal escape by confocal microscopy. MDA-MB-231 (integrin $\alpha_v\beta_3$ positive) and C4-2 cells (integrin $\alpha_v\beta_3$ negative) were seeded on 35mm glass-bottom petri dishes (MatTeck Corp) at a density of $2x10^4$ cells/well for 24 hours. Complexes of Cy5-siRNA/dual-RGD or Cy5-siRNA/dsRBD-18His at 0.5 µM were added to the culture media for 6 h. Lysotracker Green DND-26 (80nM) and DAPI (0.2µg/ml) were added into the culture media for 2 h. Images were captured on a confocal laser scanning microscope (LSM 510, Carl Zeiss, Germany).

Tumor-targeting and biodistribution. 5-week-old female athymic nu/nu mice were injected with MDA-MB-231 cells ($5 x10^6$) mixed with Matrigel (v/v 1:1) (Corning, NY) subcutaneously at the back. After 4 weeks, tumor-bearing mice were tail-vein injected with 100µl of Cy5-EGFR siRNA/dual-RGD complex (5 nmoles) or equal moles of Cy5-siRNA/dsRBD-18His complex. At time points of 3h, 6h, 12h and 24h, Cy5 florescence signal of mice were detected with Xenogen IVIS100 imaging system to monitor siRNA distribution in whole body.

In vivo gene knockdown. MDA-MB-231 tumor bearing mice (n=5 per group) were iv treated with saline, EGFR siRNA only, EGFR siRNA/ dsRBD-18His, or EGFR siRNA/dual-RGD twice a week for four weeks. 5 nmoles of siRNA were added into each group. Molar ratio of siRNA to dual-RGD or to dsRBD-18His is 1:1.

Cell viability. Proliferation and cytotoxicity of dual-RGD protein was quantified by measuring WST-8 formazan using Cell Counting Kit-8 (CCK-8). C4-2 and HEK293 cells in 10% FBS containing RPMI 1640 culture medium were seeded in 96-well plate at a density of $2x10^3$ in 5% CO2 incubator for 24h at 37°C. Cells were treated with

the varying concentrations of dual-RGD for 72h. CCK-8 reagent (10µl/well) was added into each well for 4 h. Absorbance was measured at 450nm on a TECAN infinite M200 microplate reader.

In vivo toxicity assay. Athymic mice (n=6 per group, 3 male and 3 female) were iv treated with saline or dual-RGD (10nmoles) or equal volume of saline twice a week for 4 weeks. Major organs were collected for histology assay.

Histology assay. Tumors and organs (spleen, lung, kidney, intestine, heart, liver, and brain) were collected and fixed with 4% paraformaldehyde. Sections (6 mm) were cut and mounted on the slides and deparaffinized in xylene and ethyl alcohol. Major organs were stained with Hematoxylin for 10 seconds and EOSIN for 30 seconds followed by dehydration. For tumor IHC assay, sections were blocked with 3% goat serum for 2h and incubated with anti-EGFR antibody (1:500). After washing, the sections were incubated with biotinylated secondary antibody (1:200) (Vector Labs, Burlingame, CA) for 1 h. Following washing, the sections were incubated with VECTASTAIN ABC reagents for 30 min. The images were captured with a Nuance fluorescence microscope with a bright field imaging system.

Statistical analysis. The results were expressed as a mean ±SD. All Data were analyzed using two-tailed Student's t-test (Graph Pad Prism) by comparing with the control group, and $P < 0.05$ was considered statistically significant.

REFERENCES

(1) Zorde Khvalevsky, E.; Gabai, R.; Rachmut, I. H.; Horwitz, E.; Brunschwig, Z.; Orbach, A.; Shemi, A.; Golan, T.; Domb, A. J.; Yavin, E.et al. Mutant KRAS is a druggable target for pancreatic cancer. *Proc Natl Acad Sci U S A* **2013,** *110* (51), 20723.

(2) Byeon, Y.; Lee, J. W.; Choi, W. S.; Won, J. E.; Kim, G. H.; Kim, M. G.; Wi, T. I.; Lee, J. M.; Kang, T. H.; Jung, I. D.et al. CD44-Targeting PLGA Nanoparticles Incorporating Paclitaxel and FAK siRNA Overcome Chemoresistance in Epithelial Ovarian Cancer. *Cancer Res* **2018,** *78* (21), 6247.

(3) Kang, J. C.; Sun, W.; Khare, P.; Karimi, M.; Wang, X.; Shen, Y.; Ober, R. J.; Ward, E. S. Engineering a HER2-specific antibody-drug conjugate to increase lysosomal delivery and therapeutic efficacy. *Nat Biotechnol* **2019,** *37* (5), 523.

(4) Jimenez Calvente, C.; Sehgal, A.; Popov, Y.; Kim, Y. O.; Zevallos, V.; Sahin, U.; Diken, M.; Schuppan, D. Specific hepatic delivery of procollagen alpha1(I) small interfering RNA in lipid-like nanoparticles resolves liver fibrosis. *Hepatology* **2015,** *62* (4), 1285.
(5) Leonard, J. N.; Schaffer, D. V. Antiviral RNAi therapy: emerging approaches for hitting a moving target. *Gene Ther* **2006,** *13* (6), 532.
(6) Turner, A. M.; Stolk, J.; Bals, R.; Lickliter, J. D.; Hamilton, J.; Christianson, D. R.; Given, B. D.; Burdon, J. G.; Loomba, R.; Stoller, J. K.et al. Hepatic-targeted RNA interference provides robust and persistent knockdown of alpha-1 antitrypsin levels in ZZ patients. *J Hepatol* **2018,** *69* (2), 378.
(7) Solomon, S. D.; Adams, D.; Kristen, A.; Grogan, M.; Gonzalez-Duarte, A.; Maurer, M. S.; Merlini, G.; Damy, T.; Slama, M. S.; Brannagan, T. H., 3rdet al. Effects of Patisiran, an RNA Interference Therapeutic, on Cardiac Parameters in Patients With Hereditary Transthyretin-Mediated Amyloidosis. *Circulation* **2019,** *139* (4), 431.
(8) Lam, J. K.; Chow, M. Y.; Zhang, Y.; Leung, S. W. siRNA Versus miRNA as Therapeutics for Gene Silencing. *Mol Ther Nucleic Acids* **2015,** *4*, e252.
(9) Elbashir, S. M.; Lendeckel, W.; Tuschl, T. RNA interference is mediated by 21- and 22-nucleotide RNAs. *Genes Dev* **2001,** *15* (2), 188.
(10) Elbashir, S. M.; Harborth, J.; Lendeckel, W.; Yalcin, A.; Weber, K.; Tuschl, T. Duplexes of 21-nucleotide RNAs mediate RNA interference in cultured mammalian cells. *Nature* **2001,** *411* (6836), 494.
(11) Leung, R. K.; Whittaker, P. A. RNA interference: from gene silencing to gene-specific therapeutics. *Pharmacol Ther* **2005,** *107* (2), 222.
(12) Bertrand, J. R.; Pottier, M.; Vekris, A.; Opolon, P.; Maksimenko, A.; Malvy, C. Comparison of antisense oligonucleotides and siRNAs in cell culture and in vivo. *Biochem Biophys Res Commun* **2002,** *296* (4), 1000.
(13) Second RNAi drug approved. *Nat Biotechnol* **2020,** *38* (4), 385.
(14) Priegue, J. M.; Crisan, D. N.; Martinez-Costas, J.; Granja, J. R.; Fernandez-Trillo, F.; Montenegro, J. In Situ Functionalized Polymers for siRNA Delivery. *Angew Chem Int Ed Engl* **2016,** *55* (26), 7492.
(15) Siegwart, D. J.; Whitehead, K. A.; Nuhn, L.; Sahay, G.; Cheng, H.; Jiang, S.; Ma, M.; Lytton-Jean, A.; Vegas, A.; Fenton, P.et al. Combinatorial synthesis of chemically diverse core-shell nanoparticles for intracellular delivery. *Proc Natl Acad Sci U S A* **2011,** *108* (32), 12996.
(16) Beloor, J.; Zeller, S.; Choi, C. S.; Lee, S. K.; Kumar, P. Cationic cell-penetrating peptides as vehicles for siRNA delivery. *Ther Deliv* **2015,** *6* (4), 491.
(17) Oe, Y.; Christie, R. J.; Naito, M.; Low, S. A.; Fukushima, S.; Toh, K.; Miura, Y.; Matsumoto, Y.; Nishiyama, N.; Miyata, K.et al. Actively-targeted polyion complex micelles stabilized by cholesterol and disulfide cross-linking for systemic delivery of siRNA to solid tumors. *Biomaterials* **2014,** *35* (27), 7887.
(18) Xue, H. Y.; Liu, S.; Wong, H. L. Nanotoxicity: a key obstacle to clinical translation of siRNA-based nanomedicine. *Nanomedicine (Lond)* **2014,** *9* (2), 295.
(19) Zhao, J.; Mi, Y.; Feng, S. S. siRNA-based nanomedicine. *Nanomedicine (Lond)* **2013,** *8* (6), 859.
(20) Liu, H. Y.; Gao, X. A universal protein tag for delivery of SiRNA-aptamer chimeras. *Sci Rep* **2013,** *3*, 3129.
(21) Ucci, J. W.; Kobayashi, Y.; Choi, G.; Alexandrescu, A. T.; Cole, J. L. Mechanism of interaction of the double-stranded RNA (dsRNA) binding domain of protein kinase R with short dsRNA sequences. *Biochemistry* **2007,** *46* (1), 55.
(22) Bevilacqua, P. C.; Cech, T. R. Minor-groove recognition of double-stranded RNA by the double-stranded RNA-binding domain from the RNA-activated protein kinase PKR. *Biochemistry* **1996,** *35* (31), 9983.
(23) Han, X.; Cheng, K.; Xu, Y.; Wang, Y.; Min, H.; Zhang, Y.; Zhao, X.; Zhao, R.; Anderson, G. J.; Ren, L.et al. Modularly Designed Peptide Nanoprodrug Augments Antitumor Immunity of PD-L1 Checkpoint Blockade by Targeting Indoleamine 2,3-Dioxygenase. *J Am Chem Soc* **2020,** *142* (5), 2490.
(24) Kim, J.; Lee, S. H.; Choe, J.; Park, T. G. Intracellular small interfering RNA delivery using genetically engineered double-stranded RNA binding protein domain. *J Gene Med* **2009,** *11* (9), 804.
(25) Zhu, L.; Guo, N.; Li, Q.; Ma, Y.; Jacboson, O.; Lee, S.; Choi, H. S.; Mansfield, J. R.; Niu, G.; Chen, X. Dynamic PET and Optical Imaging and Compartment Modeling using a Dual-labeled Cyclic RGD Peptide Probe. *Theranostics* **2012,** *2* (8), 746.
(26) Li, Z. B.; Chen, K.; Chen, X. (68)Ga-labeled multimeric RGD peptides for microPET imaging of integrin alpha(v)beta (3) expression. *Eur J Nucl Med Mol Imaging* **2008,** *35* (6), 1100.

(27) Kang, F.; Wang, Z.; Li, G.; Wang, S.; Liu, D.; Zhang, M.; Zhao, M.; Yang, W.; Wang, J. Inter-heterogeneity and intra-heterogeneity of alphavbeta3 in non-small cell lung cancer and small cell lung cancer patients as revealed by (68)Ga-RGD2 PET imaging. *Eur J Nucl Med Mol Imaging* **2017,** *44* (9), 1520.
(28) Cao, L.; Du, P.; Jiang, S. H.; Jin, G. H.; Huang, Q. L.; Hua, Z. C. Enhancement of antitumor properties of TRAIL by targeted delivery to the tumor neovasculature. *Mol Cancer Ther* **2008,** *7* (4), 851.
(29) Sun, Y.; Kang, C.; Liu, F.; Zhou, Y.; Luo, L.; Qiao, H. RGD Peptide-Based Target Drug Delivery of Doxorubicin Nanomedicine. *Drug Dev Res* **2017,** *78* (6), 283.
(30) Jin, Z. H.; Furukawa, T.; Degardin, M.; Sugyo, A.; Tsuji, A. B.; Yamasaki, T.; Kawamura, K.; Fujibayashi, Y.; Zhang, M. R.; Boturyn, D.et al. alphaVbeta3 Integrin-Targeted Radionuclide Therapy with 64Cu-cyclam-RAFT-c(-RGDfK-)4. *Mol Cancer Ther* **2016,** *15* (9), 2076.
(31) Wang, H.; Chen, K.; Cai, W.; Li, Z.; He, L.; Kashefi, A.; Chen, X. Integrin-targeted imaging and therapy with RGD4C-TNF fusion protein. *Mol Cancer Ther* **2008,** *7* (5), 1044.
(32) Pierschbacher, M. D.; Ruoslahti, E. Cell attachment activity of fibronectin can be duplicated by small synthetic fragments of the molecule. *Nature* **1984,** *309* (5963), 30.
(33) Pierschbacher, M.; Hayman, E. G.; Ruoslahti, E. Synthetic peptide with cell attachment activity of fibronectin. *Proc Natl Acad Sci U S A* **1983,** *80* (5), 1224.
(34) Kim, I.; Liu, C. W.; Puglisi, J. D. Specific recognition of HIV TAR RNA by the dsRNA binding domains (dsRBD1-dsRBD2) of PKR. *J Mol Biol* **2006,** *358* (2), 430.
(35) Liu, H. Y.; Yu, X.; Liu, H.; Wu, D.; She, J. X. Co-targeting EGFR and survivin with a bivalent aptamer-dual siRNA chimera effectively suppresses prostate cancer. *Sci Rep* **2016,** *6*, 30346.
(36) Yu, X.; Ghamande, S.; Liu, H.; Xue, L.; Zhao, S.; Tan, W.; Zhao, L.; Tang, S. C.; Wu, D.; Korkaya, H.et al. Targeting EGFR/HER2/HER3 with a Three-in-One Aptamer-siRNA Chimera Confers Superior Activity against HER2(+) Breast Cancer. *Mol Ther Nucleic Acids* **2018,** *10*, 317.
(37) Yamada, S.; Bu, X. Y.; Khankaldyyan, V.; Gonzales-Gomez, I.; McComb, J. G.; Laug, W. E. Effect of the angiogenesis inhibitor Cilengitide (EMD 121974) on glioblastoma growth in nude mice. *Neurosurgery* **2006,** *59* (6), 1304.
(38) Burke, P. A.; DeNardo, S. J.; Miers, L. A.; Lamborn, K. R.; Matzku, S.; DeNardo, G. L. Cilengitide targeting of alpha(v)beta(3) integrin receptor synergizes with radioimmunotherapy to increase efficacy and apoptosis in breast cancer xenografts. *Cancer Res* **2002,** *62* (15), 4263.
(39) Eguchi, A.; Meade, B. R.; Chang, Y. C.; Fredrickson, C. T.; Willert, K.; Puri, N.; Dowdy, S. F. Efficient siRNA delivery into primary cells by a peptide transduction domain-dsRNA binding domain fusion protein. *Nat Biotechnol* **2009,** *27* (6), 567.
(40) Clemens, M. J.; Elia, A. The double-stranded RNA-dependent protein kinase PKR: structure and function. *J Interferon Cytokine Res* **1997,** *17* (9), 503.
(41) Chong, K. L.; Feng, L.; Schappert, K.; Meurs, E.; Donahue, T. F.; Friesen, J. D.; Hovanessian, A. G.; Williams, B. R. Human p68 kinase exhibits growth suppression in yeast and homology to the translational regulator GCN2. *EMBO J* **1992,** *11* (4), 1553.
(42) St Johnston, D.; Brown, N. H.; Gall, J. G.; Jantsch, M. A conserved double-stranded RNA-binding domain. *Proc Natl Acad Sci U S A* **1992,** *89* (22), 10979.
(43) Green, S. R.; Mathews, M. B. Two RNA-binding motifs in the double-stranded RNA-activated protein kinase, DAI. *Genes Dev* **1992,** *6* (12B), 2478.
(44) Meurs, E.; Chong, K.; Galabru, J.; Thomas, N. S.; Kerr, I. M.; Williams, B. R.; Hovanessian, A. G. Molecular cloning and characterization of the human double-stranded RNA-activated protein kinase induced by interferon. *Cell* **1990,** *62* (2), 379.
(45) Lee, K.; Kunkeaw, N.; Jeon, S. H.; Lee, I.; Johnson, B. H.; Kang, G. Y.; Bang, J. Y.; Park, H. S.; Leelayuwat, C.; Lee, Y. S. Precursor miR-886, a novel noncoding RNA repressed in cancer, associates with PKR and modulates its activity. *RNA* **2011,** *17* (6), 1076.
(46) Gal-Ben-Ari, S.; Barrera, I.; Ehrlich, M.; Rosenblum, K. PKR: A Kinase to Remember. *Front Mol Neurosci* **2018,** *11*, 480.
(47) Hunter, T.; Hunt, T.; Jackson, R. J.; Robertson, H. D. The characteristics of inhibition of protein synthesis by double-stranded ribonucleic acid in reticulocyte lysates. *The Journal of biological chemistry* **1975,** *250* (2), 409.

(48) Estrella, V.; Chen, T.; Lloyd, M.; Wojtkowiak, J.; Cornnell, H. H.; Ibrahim-Hashim, A.; Bailey, K.; Balagurunathan, Y.; Rothberg, J. M.; Sloane, B. F.et al. Acidity generated by the tumor microenvironment drives local invasion. *Cancer Res* **2013,** *73* (5), 1524.
(49) Huotari, J.; Helenius, A. Endosome maturation. *EMBO J* **2011,** *30* (17), 3481.
(50) Creusat, G.; Rinaldi, A. S.; Weiss, E.; Elbaghdadi, R.; Remy, J. S.; Mulherkar, R.; Zuber, G. Proton sponge trick for pH-sensitive disassembly of polyethylenimine-based siRNA delivery systems. *Bioconjug Chem* **2010,** *21* (5), 994.
(51) Tai, W.; Li, J.; Corey, E.; Gao, X. Publisher Correction: A ribonucleoprotein octamer for targeted siRNA delivery. *Nat Biomed Eng* **2018,** *2* (8), 622.
(52) Prokopiou, E. M.; Ryder, S. A.; Walsh, J. J. Tumour vasculature targeting agents in hybrid/conjugate drugs. *Angiogenesis* **2013,** *16* (3), 503.
(53) Desgrosellier, J. S.; Cheresh, D. A. Integrins in cancer: biological implications and therapeutic opportunities. *Nat Rev Cancer* **2010,** *10* (1), 9.
(54) Cooper, C. R.; Chay, C. H.; Pienta, K. J. The role of alpha(v)beta(3) in prostate cancer progression. *Neoplasia* **2002,** *4* (3), 191.
(55) Zhao, Y.; Bachelier, R.; Treilleux, I.; Pujuguet, P.; Peyruchaud, O.; Baron, R.; Clement-Lacroix, P.; Clezardin, P. Tumor alphavbeta3 integrin is a therapeutic target for breast cancer bone metastases. *Cancer Res* **2007,** *67* (12), 5821.
(56) Wang, F.; Li, Y.; Shen, Y.; Wang, A.; Wang, S.; Xie, T. The functions and applications of RGD in tumor therapy and tissue engineering. *Int J Mol Sci* **2013,** *14* (7), 13447.
(57) Klubo-Gwiezdzinska, J.; Chen, X. Targeting Integrins with Radiolabeled RGD Analogues for Radiotheranostics of Metastatic Radioactive Iodine Nonresponsive Thyroid Cancer: New Avenues in Personalized Medicine. *Thyroid* **2020,** *30* (4), 476.
(58) Doss, M.; Kolb, H. C.; Zhang, J. J.; Belanger, M. J.; Stubbs, J. B.; Stabin, M. G.; Hostetler, E. D.; Alpaugh, R. K.; von Mehren, M.; Walsh, J. C.et al. Biodistribution and radiation dosimetry of the integrin marker 18F-RGD-K5 determined from whole-body PET/CT in monkeys and humans. *J Nucl Med* **2012,** *53* (5), 787.
(59) Chen, H.; Niu, G.; Wu, H.; Chen, X. Clinical Application of Radiolabeled RGD Peptides for PET Imaging of Integrin alphavbeta3. *Theranostics* **2016,** *6* (1), 78.
(60) Pasqualini, R.; Koivunen, E.; Kain, R.; Lahdenranta, J.; Sakamoto, M.; Stryhn, A.; Ashmun, R. A.; Shapiro, L. H.; Arap, W.; Ruoslahti, E. Aminopeptidase N is a receptor for tumor-homing peptides and a target for inhibiting angiogenesis. *Cancer Res* **2000,** *60* (3), 722.
(61) Hood, J. D.; Bednarski, M.; Frausto, R.; Guccione, S.; Reisfeld, R. A.; Xiang, R.; Cheresh, D. A. Tumor regression by targeted gene delivery to the neovasculature. *Science* **2002,** *296* (5577), 2404.
(62) Harris, T. D.; Kalogeropoulos, S.; Nguyen, T.; Liu, S.; Bartis, J.; Ellars, C.; Edwards, S.; Onthank, D.; Silva, P.; Yalamanchili, P.et al. Design, synthesis, and evaluation of radiolabeled integrin alpha v beta 3 receptor antagonists for tumor imaging and radiotherapy. *Cancer Biother Radiopharm* **2003,** *18* (4), 627.
(63) Janssen, M. L.; Oyen, W. J.; Dijkgraaf, I.; Massuger, L. F.; Frielink, C.; Edwards, D. S.; Rajopadhye, M.; Boonstra, H.; Corstens, F. H.; Boerman, O. C. Tumor targeting with radiolabeled alpha(v)beta(3) integrin binding peptides in a nude mouse model. *Cancer Res* **2002,** *62* (21), 6146.
(64) Zhang, Y. F.; Wang, J. C.; Bian, D. Y.; Zhang, X.; Zhang, Q. Targeted delivery of RGD-modified liposomes encapsulating both combretastatin A-4 and doxorubicin for tumor therapy: in vitro and in vivo studies. *Eur J Pharm Biopharm* **2010,** *74* (3), 467.
(65) Wang, K.; Zhang, X.; Zhang, L.; Qian, L.; Liu, C.; Zheng, J.; Jiang, Y. Development of biodegradable polymeric implants of RGD-modified PEG-PAMAM-DOX conjugates for long-term intratumoral release. *Drug Deliv* **2015,** *22* (3), 389.
(66) Bertilaccio, M. T.; Grioni, M.; Sutherland, B. W.; Degl'Innocenti, E.; Freschi, M.; Jachetti, E.; Greenberg, N. M.; Corti, A.; Bellone, M. Vasculature-targeted tumor necrosis factor-alpha increases the therapeutic index of doxorubicin against prostate cancer. *Prostate* **2008,** *68* (10), 1105.
(67) Corti, A.; Ponzoni, M. Tumor vascular targeting with tumor necrosis factor alpha and chemotherapeutic drugs. *Ann N Y Acad Sci* **2004,** *1028*, 104.

ACKNOWLEDGEMENT

This work is supported by start-up funding of Augusta University and NIH R21EB026564-01A (to H.Y.L.).

AUTHOR CONTRIBUTIONS

H.Y.L. conceived and designed the experiments, H.Y.L., X.Y., L.X, J.Z performed the experiments. H.Y.L., X.Y.

L.X. S.Z D.W. analyzed the data. H.Y.L. S.Z and D.W. wrote the manuscript.

COMPETING INTERESTS

Authors do not have any competing interests to declare.

Supplementary Files

This is a list of supplementary files associated with this preprint. Click to download.

- Supplementaryinformation.pdf